

# UC Berkeley

## UC Berkeley Previously Published Works

### Title

Asymmetric emergence of low-to-no snow in the midlatitudes of the American Cordillera

### Permalink

<https://escholarship.org/uc/item/1rh5s5bh>

### Journal

Nature Climate Change, 12(12)

### ISSN

1758-678X

### Authors

Rhoades, Alan M

Hatchett, Benjamin J

Risser, Mark D

et al.

### Publication Date

2022-12-01

### DOI

10.1038/s41558-022-01518-y

### Copyright Information

This work is made available under the terms of a Creative Commons Attribution License, available at <https://creativecommons.org/licenses/by/4.0/>

Peer reviewed

# Asymmetric emergence of low-to-no snow in the midlatitudes of the American Cordillera

Received: 14 October 2021

Accepted: 7 October 2022

Published online: 14 November 2022

 Check for updates

Alan M. Rhoades<sup>1</sup>✉, Benjamin J. Hatchett<sup>2</sup>, Mark D. Risser<sup>1</sup>, William D. Collins<sup>1,3</sup>, Nicolas E. Bambach<sup>4</sup>, Laurie S. Huning<sup>5,6</sup>, Rachel McCrary<sup>7</sup>, Erica R. Siirila-Woodburn<sup>8</sup>, Paul A. Ullrich<sup>1,4</sup>, Michael F. Wehner<sup>9</sup>, Colin M. Zarzycki<sup>10</sup> & Andrew D. Jones<sup>1,11</sup>

Societies and ecosystems within and downstream of mountains rely on seasonal snowmelt to satisfy their water demands. Anthropogenic climate change has reduced mountain snowpacks worldwide, altering snowmelt magnitude and timing. Here the global warming level leading to widespread and persistent mountain snowpack decline, termed low-to-no snow, is estimated for the world's most latitudinally contiguous mountain range, the American Cordillera. We show that a combination of dynamical, thermodynamical and hypsometric factors results in an asymmetric emergence of low-to-no-snow conditions within the midlatitudes of the American Cordillera. Low-to-no-snow emergence occurs approximately 20 years earlier in the southern hemisphere, at a third of the local warming level, and coincides with runoff efficiency declines (8% average) in both dry and wet years. The prevention of a low-to-no-snow future in either hemisphere requires the level of global warming to be held to, at most, +2.5 °C.

Mountains comprise 12% of the global land area outside of Antarctica, but they disproportionately influence atmospheric, hydrologic and cryospheric processes across a continuum of spatio-temporal scales<sup>1</sup>. Through orographic enhancement of precipitation, mountains extract moisture from the atmosphere and store portions of this water in the form of seasonal snow, glaciers, surface water, soil moisture and groundwater<sup>2–6</sup>. As a result, mountain-derived water supports approximately 22% of the world's water resource needs<sup>7</sup>.

The American Cordillera is the most latitudinally contiguous mountain range in the world<sup>8</sup>. The land-surface characteristics and hydrologic cycles in the midlatitudes of the American Cordillera have often been described as distorted mirror images of one another, on the basis of regional atmosphere and ocean circulations<sup>9</sup>, comparable storm types (for example, atmospheric rivers<sup>10</sup>) and seasonal snowpack

dynamics<sup>5</sup>, which give rise to analogous ecosystems<sup>11–13</sup> yet distinct hydroclimatologies based on different mountain hypsometry. Societies in these regions need to monitor the volume of water stored as snow and the timing of snowmelt to meet water demand in productive agricultural valleys and populous urban areas<sup>7,14</sup>.

Anthropogenic climate change is expected to fundamentally alter the hydrologic cycle in mountains<sup>5,7,15,16</sup>. These alterations include phase changes in precipitation, decreased snowpack and glacial water storage, and amplified warming with increasing elevation<sup>5,17–19</sup>. To date, the combined effect of these alterations drives unprecedented aridity in the midlatitudes of the American Cordillera<sup>14,20–24</sup>. Coinciding with enhanced aridity, observations indicate with high confidence that mountain snow cover has appreciably declined<sup>25</sup>. If trends in model projections are correct, deleterious, widespread and persistent

<sup>1</sup>Climate and Ecosystem Sciences Division, Lawrence Berkeley National Laboratory, Berkeley, CA, USA. <sup>2</sup>Desert Research Institute, Reno, NV, USA.

<sup>3</sup>Department of Earth and Planetary Science, University of California, Berkeley, CA, USA. <sup>4</sup>Department of Land, Air, and Water Resources, University of California, Davis, CA, USA. <sup>5</sup>Department of Civil Engineering and Construction Engineering Management, California State University, Long Beach, CA, USA. <sup>6</sup>Department of Civil and Environmental Engineering, University of California, Irvine, CA, USA. <sup>7</sup>National Center for Atmospheric Research, Boulder, CO, USA. <sup>8</sup>Energy Geosciences Division, Lawrence Berkeley National Laboratory, Berkeley, CA, USA. <sup>9</sup>Computational Research Division, Lawrence Berkeley National Laboratory, Berkeley, CA, USA. <sup>10</sup>Department of Meteorology and Atmospheric Science, Penn State University, State College, PA, USA. <sup>11</sup>Energy and Resources Group, University of California, Berkeley, Berkeley, CA, USA. ✉e-mail: [arhoades@lbl.gov](mailto:arhoades@lbl.gov)

impacts on downstream water resource availability and timing could occur across the American Cordillera<sup>18</sup>. This outcome is referred to as a low-to-no-snow future<sup>16</sup>.

Although the midlatitudes of the American Cordillera have historically shared common hydroclimatic characteristics, there is evidence in the palaeoclimate and historical record that hemispheric changes induced by climate change may be asymmetric<sup>26–30</sup>. This is due to process interactions at planetary-synoptic scales through differential alterations to the general circulation and the jet stream, which in turn influence the midlatitude storm track location, variability and persistence<sup>27,28</sup>; at meso-scales through thermodynamic changes in storm characteristics pertaining to precipitation processes (for example, Clausius–Clapeyron scaling and precipitation efficiency<sup>10</sup>) and land-surface warming and associated feedbacks<sup>17</sup>; and at micro-scales through factors associated with mountain hypsometry such as topographic height, slope and ruggedness<sup>31,32</sup>, as shown in Fig. 2 of Siirila-Woodburn et al.<sup>16</sup>.

Hemispheric asymmetries in response to anthropogenic climate change also imply that the emergence of low-to-no-snow conditions may occur at different times in the midlatitudes of the northern and southern hemispheres. This differing timing is a consequence of interactions between dynamical, thermodynamical and hypsometric factors. Midlatitude asymmetries arise through alterations in global teleconnections (for example, the El Niño Southern Oscillation<sup>33</sup>), the genesis and landfall locations of storms<sup>10</sup>, the efficiency with which mountains extract moisture from the atmosphere<sup>34</sup>, the elevation of the freezing level<sup>35</sup>, the snowfall fraction of storms<sup>36</sup>, and the evolution of snowpack cold content<sup>37</sup> that drives metamorphism and eventual snowmelt<sup>38</sup>. It is therefore imperative to understand and estimate how these process interactions influence the emergence of a low-to-no-snow future across the American Cordillera, particularly for instilling resilience into water resource management.

## Identifying low-to-no-snow emergence

The inherent issues in modelling the process interactions that shape the mountainous hydrologic cycle pose a scientific grand challenge, particularly in estimating the time horizon, spatial extent and magnitude of low-to-no-snow conditions<sup>16</sup>. Simulating decadal to centennial changes in mountain hydrology at global scales with better fidelity requires high-resolution models (that is,  $\leq 0.5^\circ$  horizontal resolution as discussed by Demory et al.<sup>39</sup>) and cannot be done with traditional Earth system model simulations<sup>40,41</sup>. However, current climate simulations may now be approaching the resolutions needed to investigate the emergence of a low-to-no-snow future in mountains at both global and regional scales<sup>42</sup>. Because it is one of the first multi-model ensembles that provide simulations at resolutions needed to capture global-scale mountain snowpack dynamics, we leverage the High Resolution Model Intercomparison Project (HighResMIP) ensemble<sup>43</sup>, which utilizes the high-emissions (SSP5-8.5) scenario<sup>44</sup>. We follow Körner et al.<sup>45</sup> in defining mountains, particularly the American Cordillera, and Siirila-Woodburn et al.<sup>16</sup> in quantitatively characterizing low-to-no-snow emergence. The latter definition is based on annual peak snow water equivalent (SWE) percentiles (Methods). Next, we assess low-to-no-snow persistence and its connection to warming, and we identify whether there is hemispheric asymmetry in the midlatitudes of the American Cordillera. Last, we detail how the mountainous hydrologic cycle is fundamentally altered following the emergence of low-to-no snow.

Over the historical period (1950–2000), interannual variability in peak SWE is high relative to average declines along the American Cordillera, representing a weak signal-to-noise ratio of snow loss (Fig. 1 and Supplementary Fig. 1). The signal of change refers to the trend in peak SWE decline, whereas the noise is the interannual variability in peak SWE magnitude. The magnitudes of peak SWE change are also provided (Supplementary Fig. 2). However, between 2025 and 2050, only

portions of the American Cordillera exhibit consistent below-median historical peak SWE percentiles. After 2050, below-median historical peak SWE percentiles are consistently projected across the American Cordillera, indicating a stronger signal-to-noise emergence (Fig. 1). This systematic emergence coincides with a divergence in hemispheric warming and associated differences in mean meridional overturning circulation, indicating differing mechanistic influences on low-to-no-snow emergence (Fig. 2). The weakening of the northern hemisphere general circulation could shape low-to-no-snow emergence through dynamically induced shifts of the midlatitude jet, which steers the storm track and drives thermodynamic controls on landfalling storm precipitation amount and phase and snowpack ripening due to an altered energy balance. In the southern hemisphere, the general circulation shows little response to warming, and low-to-no-snow emergence could be controlled primarily through thermodynamic controls.

While decreases in mean peak SWE for 2015–2050 relative to 1950–2000 are consistent and substantial in California's Sierra Nevada (4/6 simulations), the results are less consistent throughout the Pacific Northwest and North American Rockies (Supplementary Fig. 3). This result is shaped by differential changes in annual mean total precipitation (Supplementary Fig. 4) and surface air temperature within individual simulations (Supplementary Fig. 5). In the southern hemisphere, models (4/6) project increases in mean peak SWE (Supplementary Fig. 6). This results from increases in annual mean total precipitation (Supplementary Fig. 7) combined with weaker, though substantial, annual mean surface air temperature increases compared with the northern hemisphere (Supplementary Fig. 8). However, a notable decrease in mean peak SWE in both hemispheres is found by the two models that project out to 2100, save for certain portions of the Canadian Rockies and northern Chilean Andes (Supplementary Figs. 3d,e and 6d,e).

Although Fig. 1 demonstrates a transition from average snow conditions to a future of low-to-no snow, it does not enable precise isolation of the emergence and persistence of snow loss given the difficulties in identifying a trend signal between 1950 and 2050. Hereafter, we focus our analysis on the highest-resolution model simulation (20 km, MRI-AGCM3-2-S) of the two available 150-year projections (1950–2099) in the HighResMIP ensemble to investigate the date of and degrees to emergence of low-to-no snow within the American Cordillera. It is important to note that our threshold-based approach imposes a threshold categorization ( $\leq 30$ th percentile historical peak SWE) of individual years as low-to-no-snow years, which obscures both the continuous nature of snowpack decline and the presence of various context-specific physical and infrastructural nonlinearities and thresholds at which impacts occur. The percentile-based threshold was chosen to be of sufficient magnitude to represent meaningful physical changes and societal impacts associated with snow prevalence<sup>16</sup>, and it enables us to use a consistent approach for examining the timing and drivers of low-to-no-snow emergence across geographic regions. To isolate the date at which snowpack depletion begins to appreciably impact the mountainous hydrologic cycle, we define thresholds for low-to-no-snow conditions at three different sequential time periods (Methods): extreme (back-to-back low-to-no-snow years), episodic (low-to-no snow conditions spanning five years) and persistent (low-to-no snow conditions spanning ten years). To identify midlatitude asymmetry in the emergence of low-to-no snow conditions, we use common latitude bands of  $\pm 32$ – $59^\circ$ . These latitude bands are symmetric about one another and comprise mountainous regions that maintain seasonal snowpacks across the entire 150-year period (as indicated by the extensive amount of missing values and/or more ephemeral snow conditions between the latitude bands of  $\pm 0$ – $32^\circ$  in Fig. 1b). The hemispheric-wide emergence of extreme low-to-no-snow conditions occurs 17 years earlier in the southern hemisphere with a median date of 2039<sup>2051</sup><sub>2015</sub> (standard median 95% confidence intervals are provided as a superscript and subscript<sup>46</sup>), versus 2056<sup>2062</sup><sub>2049</sub> in the northern hemisphere (Fig. 3a,c). This midlatitude asymmetry in low-to-no-snow

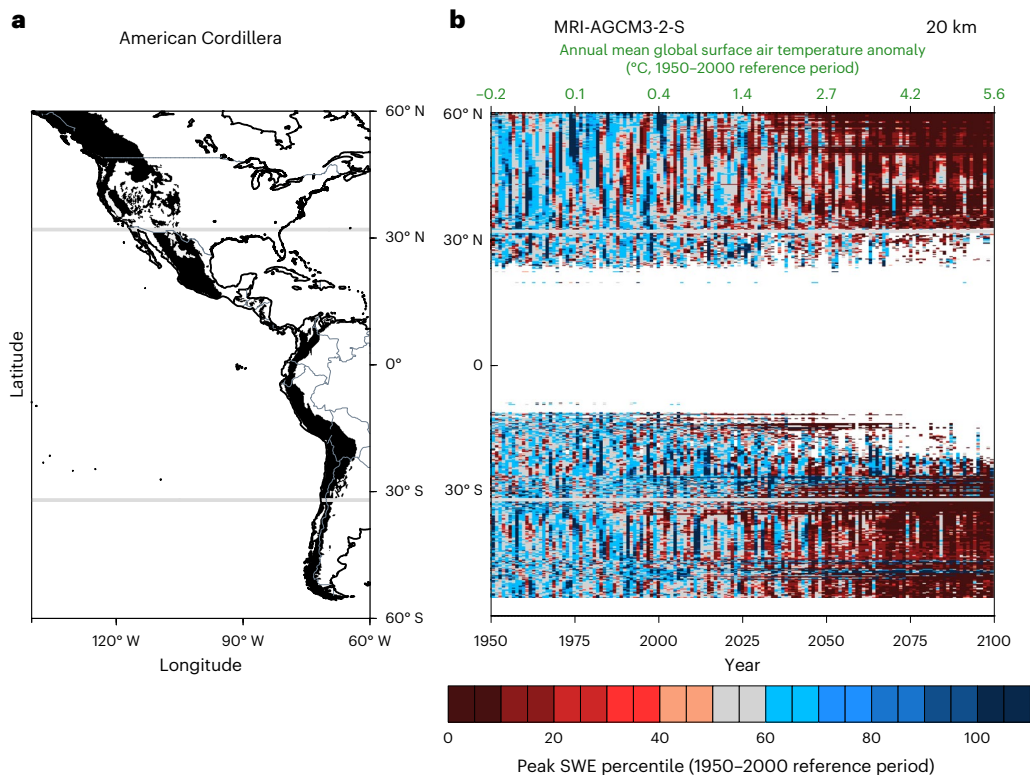


**Fig. 1 | The signal-to-noise ratio of low-to-no-snow emergence.** **a**, American Cordillera (black polygons) from 60° N to 60° S. Lines at  $\pm 32^\circ$  latitude and country borders are shown in grey. **b**, Latitude band averages of annual peak SWE percentiles within the American Cordillera as simulated by the highest-resolution (20 km) HighResMIP simulation (MRI-AGCM3-2-S) over 1950–2100 under the high-emissions shared socio-economic pathway (SSP5-8.5). The top

x axis shows the annual mean global surface air temperature anomalies, and the bottom x axis indicates the years between 1950 and 2100. The years 1950–2000 are used as the historical reference period to compute percentile bins and annual mean temperature anomalies. White regions indicate annual peak SWE values  $\leq 2.54$  mm or no SWE. Low-to-no-snow conditions are defined as latitude band average annual peak SWE  $\leq 30$ th percentile.

emergence timing is approximately the same for the episodic threshold (with a hemispheric difference of 19 years) and the persistent threshold (with a hemispheric difference of 22 years). Given the convergence in the median date of emergence of low-to-no-snow conditions between the episodic and persistent thresholds (Fig. 3a,c), post-emergence of low-to-no snow is hereafter defined as all years following the emergence of episodic low-to-no snow, or 2051<sub>2046</sub><sup>2051</sup> in the southern hemisphere and 2070<sub>2065</sub><sup>2073</sup> in the northern hemisphere.

The northern hemisphere, consistent with Xu and Ramanathan<sup>27</sup> and Friedman et al.<sup>28</sup>, warms faster than the southern hemisphere (Fig. 2a), even within the American Cordillera (Fig. 2b). Low-to-no-snow emergence occurs at a median local surface air temperature change of  $+3.5^{+4.0}_{+3.4}$  °C relative to 1950–2000. In the southern hemisphere, this occurs with approximately a third of the local warming,  $+1.2^{+1.2}_{+0.9}$  °C (Fig. 3b,d). This difference is partly explained by the historically warmer local annual surface air temperatures in the mountainous regions of the southern hemisphere (median of 5.7 °C over 1950–2000) than in the northern hemisphere (median of 2.7 °C over 1950–2000). From a global warming perspective, low-to-no-snow emergence occurs between  $+2.4$  °C and  $+2.9$  °C (between 2046 and 2051) in the southern hemisphere and between  $+3.5$  °C and  $+4.1$  °C (between 2065 and 2073) in the northern hemisphere. Elevation-dependent warming is also asymmetric (Supplementary Fig. 11a,e). The midlatitudes of the northern hemisphere experience higher elevation-dependent warming ( $+3.8$  °C per 500 m to  $+5.6$  °C per 500 m) than those of the southern hemisphere ( $+1.7$  °C per 500 m to  $+4.2$  °C per 500 m). Despite the asymmetric increase in surface air temperature in the midlatitudes of the northern hemisphere and the inclusion of both continental and maritime mountains within the American Cordillera relative to the southern

hemisphere, the net result is symmetric convergence in hemispheric median annual surface air temperatures ( $-7$ – $7.5$  °C) during the years following low-to-no-snow emergence.

### Post-emergence implications of low-to-no snow

Although midlatitude symmetry in annual mean surface air temperatures in the American Cordillera occurs over the years post-emergence of low-to-no snow (Fig. 4a), asymmetric mountain hydrologic cycle responses arise. This reflects shifts in both annual mean total precipitation (Fig. 4b) and the fraction of precipitation falling as snow, or snowfall fraction (Fig. 4c). During the historical baseline period, southern hemisphere mountains received more than twice as much precipitation (median of 3,000 mm) as the northern hemisphere (median of 1,300 mm). Yet, the change in total precipitation is more consistent in sign with latitude in the southern hemisphere following the emergence of low-to-no snow (median of  $-9\%$ ). Historically, the southern hemisphere also received a smaller fraction of precipitation as snowfall (median of 12%) than the northern hemisphere (median of 35%), but the net decline in snowfall fraction is comparable (median of  $-42\%$ ) following the emergence of low-to-no snow (Fig. 4c). In the northern hemisphere, the precipitation that falls on the surface without antecedent snow cover increases from 45% to 67% of the total precipitation fraction (Supplementary Fig. 12). In the southern hemisphere, the precipitation that falls on the surface without pre-existing snow cover increases by only 10% (73% to 83%) but still remains higher than in the northern hemisphere. This coincides with a marked decrease in the mean number of freezing days from 137 to 83 and 65 to 34 in the northern and southern hemispheres, respectively. Freezing day shifts result in changes in the percentage of total precipitation that comes as

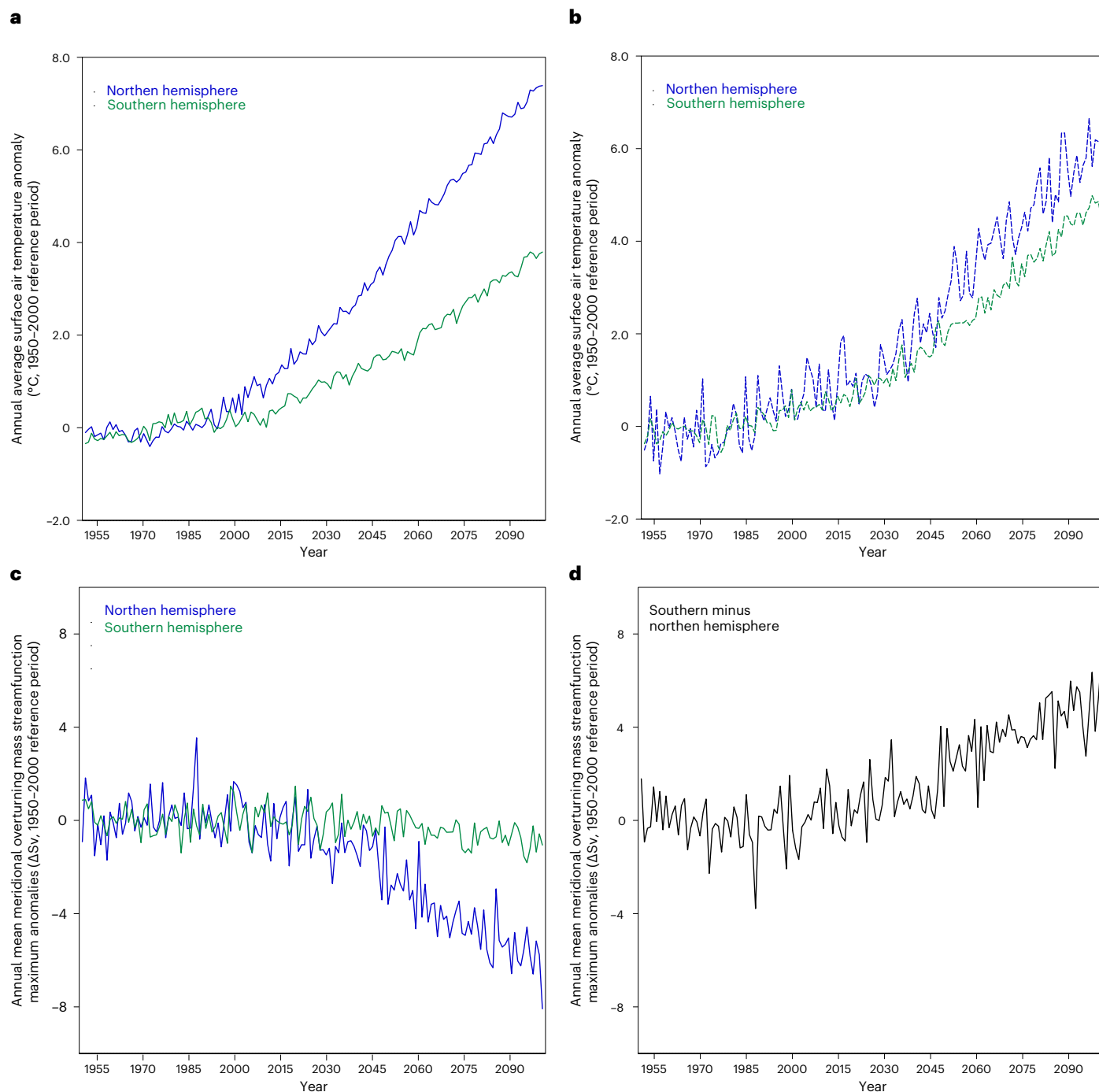


**Fig. 2 | Hemispheric asymmetry in warming and circulation changes.**

**a**, Northern (blue) and southern (green) hemisphere annual mean surface air temperature anomalies simulated by MRI-AGCM3-2-S. The years 1950–2000 are used as the historical reference period. **b**, Changes in only the American

Cordillera. **c**, The difference in annual mean maximum meridional overturning mass streamfunction from the historical reference period, with analogous methods to Friedman et al.<sup>28</sup>. **d**, The circulation differences between hemispheres (southern minus northern) in **c**.

snowfall on pre-existing snow cover from 43% to 24% in the northern hemisphere and from 21% to 14% in the southern hemisphere and a marked decrease in the area of freezing conditions and snow on both intra- and inter-annual timescales (Supplementary Figs. 13 and 14).

The combined effect of warmer surface air temperatures, increased rainfall and less snowpack post-emergence of low-to-no snow alters runoff generation in mountains (Supplementary Figs. 9–11, 13 and 14). Runoff efficiency relates the amounts of total precipitation and total runoff in a given year (Fig. 4d). Temperature strongly

dictates changes in runoff efficiency<sup>47</sup> through changes in evaporative demand<sup>23,48</sup> and seasonal snowpack amounts, which acts as a more efficient and predictable runoff generator than rainfall<sup>49–51</sup>. Specifically, warming has been shown to modulate snowmelt rate and timing, which in turn strongly influences runoff efficiency<sup>52–54</sup>. In the mid-latitudes of the northern hemisphere, a clear monotonic relationship between latitude and runoff efficiency exists over the historical period (Fig. 4d). This relationship is not as evident in the southern hemisphere (Fig. 4d). Despite the weaker relationship between runoff efficiency



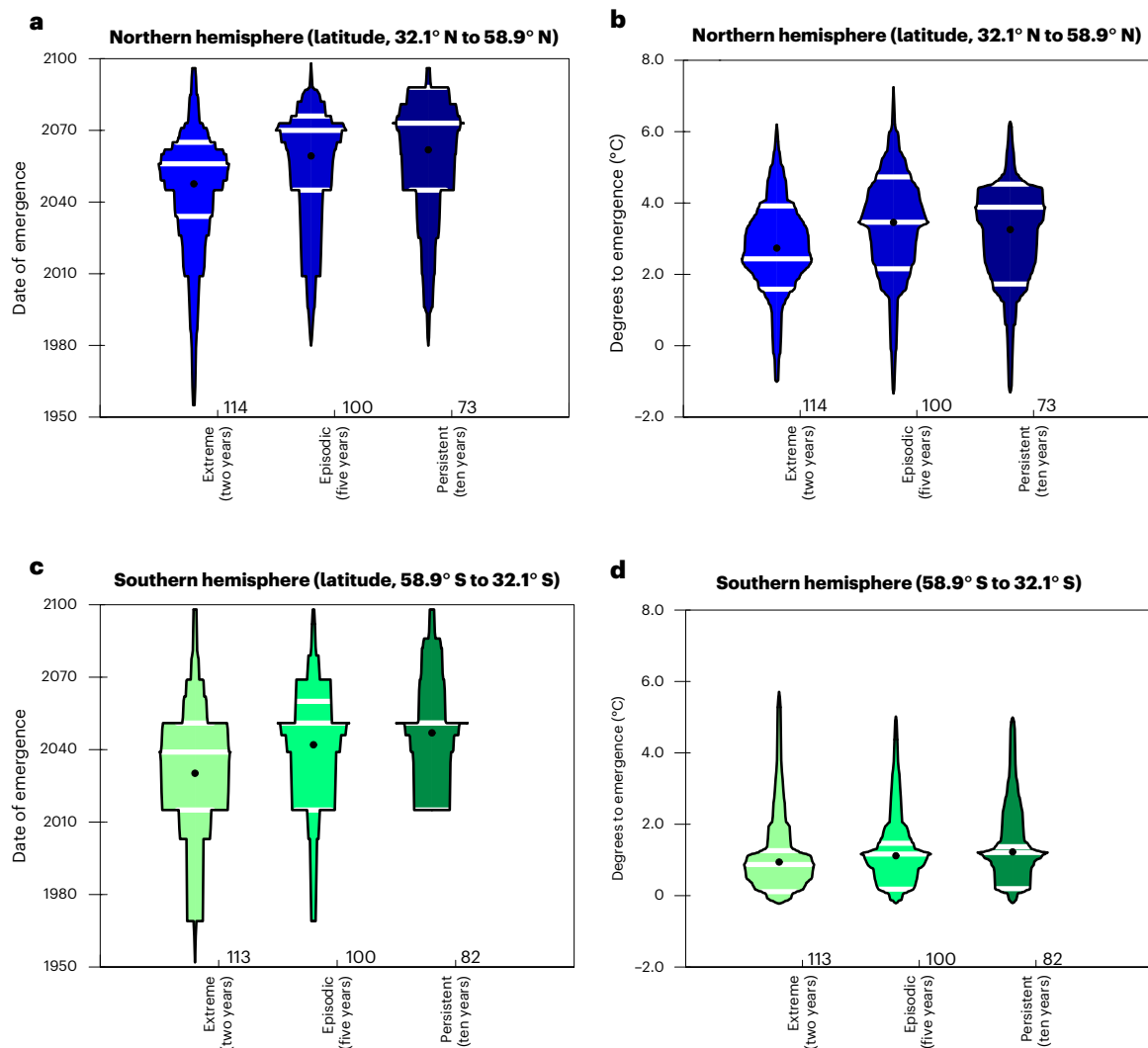


**Fig. 3 | Date of and degrees to emergence of low-to-no snow. a–d,** Box percentile plots of the latitude band average date of emergence of low-to-no snow ( $\leq 30$ th percentile historical peak SWE; 1950–2000 historical reference period) for the northern (blue;  $32^{\circ}$  N to  $59^{\circ}$  N) and southern (green;  $32^{\circ}$  S to  $59^{\circ}$  S) midlatitude portions of the American Cordillera. The white lines indicate the 75th, median and 25th percentiles, and the black circles represent the mean. The numbers along the x axis indicate the number of latitude bands that make up the

box percentile plot distributions. The date of emergence (a,c) is predicated on back-to-back years of low-to-no snow under three conditions: extreme (at least two years), episodic (at least five years) and persistent (at least ten years). The degrees to emergence (b,d) are local, annual surface air temperature changes from the 1950–2000 reference period at which extreme, episodic and persistent low-to-no-snow conditions first occur at a particular latitude band.

and latitude in the southern midlatitudes, there is a more consistent amount of historical runoff efficiency across latitudes (median of 70% versus 49% in the northern hemisphere). This relationship could be due to differences in mountain slope (higher throughout the southern hemisphere) and glacial and vegetation distributions with elevation (less in the southern hemisphere). Post-emergence of low-to-no snow, the northern midlatitudes exhibit a consistent decrease in runoff efficiency (median of  $-11\%$ ), whereas in the southern midlatitudes a more heterogeneous response occurs, with increases or decreases generally demarcated above or below latitude  $44^{\circ}$  S, respectively. This coincides with earlier peak SWE timing, slower snowmelt rates and shorter snow season lengths (Supplementary Fig. 15), corroborating the findings of Trujillo and Molotch<sup>52</sup> and Musselman et al.<sup>53</sup>. Runoff efficiency also decreases (or does not change) with elevation in the northern midlatitudes, whereas in the southern midlatitudes elevations below 3,000 m show a decrease in runoff efficiency and elevations above 3,000 m show an increase (Supplementary Fig. 11d,h). We hypothesize that this is probably a signature of glacial decline

and/or extreme storm events that impact higher elevations in the southern hemisphere<sup>55</sup>.

Despite increases in runoff efficiency with latitude (Figs. 4d and 5a,d), the spatial patterns of historic runoff efficiency also demonstrate the influence of continentality (Fig. 5a) in the northern hemisphere, with coastal mountains yielding higher runoff efficiency. Midlatitude mountain regions in both hemispheres are projected to undergo declines in runoff efficiency as a result of warming (Fig. 5b,f). The largest changes are projected for the interior Rocky Mountains (Fig. 5b) and the central Andes (Fig. 5e). Exceptions occur in the coastal ranges of British Columbia and Patagonia, where glacial melt will increase runoff, as well as in California, the southern Cascades and the northern Andes, where extreme precipitation is projected to increase<sup>55–57</sup>. As a result of warming and the emergence of low-to-no snow conditions in the late twenty-first century, we consider two types of years to examine runoff changes: (1) low-snow and low-precipitation years and (2) high-precipitation years. In the colder historical climate, low-snow years are tied more directly to low precipitation. In the future, precipitation variability and snowpack

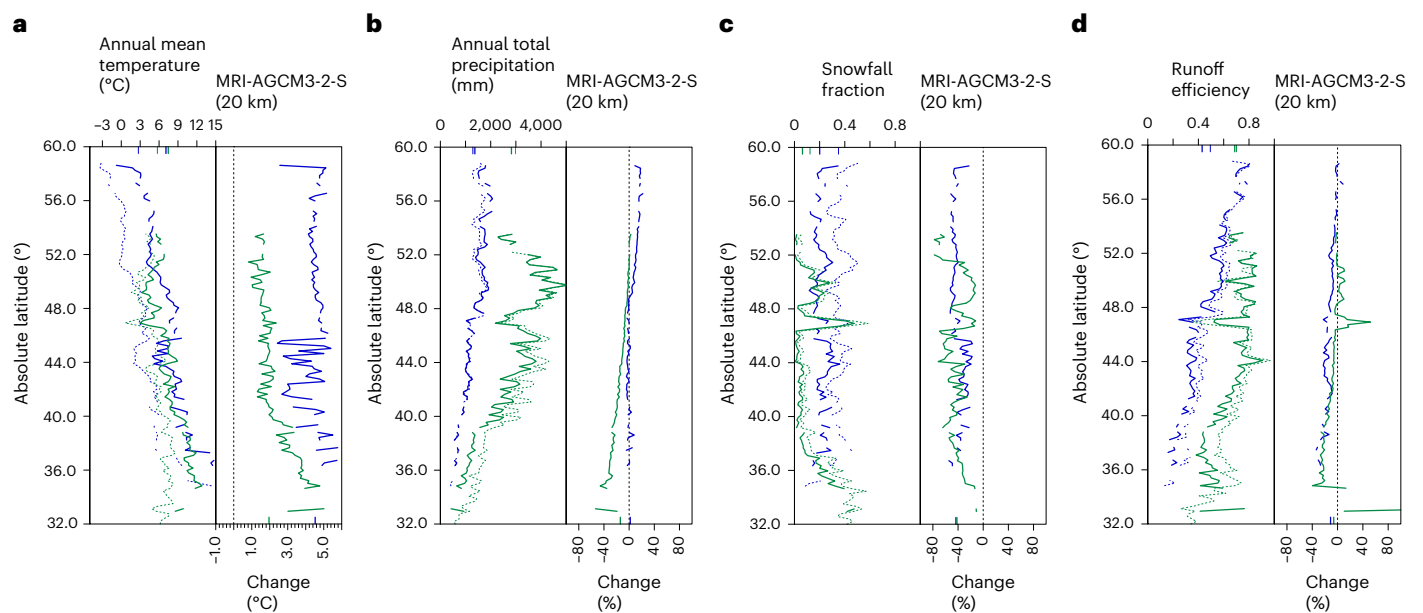


**Fig. 4 | Mountainous hydrologic cycle changes post-emergence of low-to-no snow. a–d.** Latitude band mean hydrologic cycle responses within the northern (blue) and southern (green) midlatitudes of the American Cordillera for all years following low-to-no snow emergence. The annual mean surface air temperature (a), annual mean total precipitation (b), annual mean snowfall fraction (total annual snowfall divided by total annual precipitation) (c) and annual mean runoff efficiency (total annual runoff divided by total annual precipitation) (d)

and their changes for all years post-emergence of low-to-no snow (right side of each panel) are shown. The changes are all relative to the 1950–2000 historical reference period. Historical values are shown with dashed lines. Midlatitude-wide median values for both the historical period and post-emergence of low-to-no snow are shown via coloured tick marks along the x axes. A dashed zero line is also provided in each subplot showing hydrologic cycle changes post-emergence of low-to-no snow relative to the historical reference period.

variability become more uncoupled. Declines in runoff efficiency during low-snow and low-precipitation years are the greatest in the North American Rockies (Fig. 5c) and central Andes (Fig. 5g). Runoff efficiency also decreases during future wet years (Fig. 5d,h), with exceptions in the aforementioned regions where extreme precipitation is projected to become more frequent. Runoff decreases probably result from increases in atmospheric demand for water throughout the year and a future limit on evaporation associated with less snowpack and soil moisture in drier months<sup>21</sup>. These results suggest a net reduction in the capability of American Cordillera midlatitude mountains to reliably provide water resources to downstream users post-emergence of low-to-no snow conditions.

## Discussion

Partially because the hydrologic cycles in the midlatitudes of the American Cordillera have historically been distorted mirror images of one another, their projected response to climate change is asymmetric. We found midlatitude asymmetries in the emergence of low-to-no snow conditions, or when snow loss becomes deleterious, widespread and persistent. Low-to-no snow emergence is projected to occur in the northern midlatitudes in 2070<sup>2073</sup><sub>2065</sub> at a local warming level of +3.5<sup>+4.0</sup><sub>+3.4</sub> °C. However, in the southern midlatitudes, low-to-no snow emergence is projected to occur in 2051<sup>2051</sup><sub>2046</sub> at a local warming level of +1.2<sup>+1.2</sup><sub>+0.9</sub> °C. This asymmetry in low-to-no snow emergence is a function of hypsometric differences not only along the midlatitudes of the American Cordillera but also across spatial scales. At planetary-synoptic scales, a shift in the atmospheric general circulation (for example, meridional slowdown in the northern hemisphere) was found and is related to asymmetric hemispheric warming (Fig. 2). At synoptic-to-meso scales, changes brought about by alterations to landfalling storm characteristics (for example, heterogeneous changes to annual total precipitation and ubiquitous reductions in snowfall fraction) and more localized elevation-dependent warming were identified. Our findings suggest that the prevention of midlatitude low-to-no

snow emergence requires global warming to be limited to, at most, +2.5 °C. It is important to emphasize that although the rain–snow partitioning scheme in MRI-AGCM3-2-S, unlike most Earth system models, accounts for temperature and humidity (Methods), the global warming level that gives rise to low-to-no snow emergence may be a conservative estimate. This is because the historical climatology was wetter and colder than several reanalysis datasets and regional observation-based gridded products (Supplementary Information). MRI-AGCM3-2-S also has a colder equilibrium climate sensitivity than other HighResMIP models (Supplementary Table 1), and low-to-no snow emergence occurs later than the multi-model average estimates derived from the North and South American Coordinated Regional Climate Downscaling Experiments (Supplementary Figs. 29 and 30).

Our low-to-no snow definition is an attempt at providing an annual, decision-relevant, location-independent, reproducible estimate of snow loss and its impacts. We recognize that this definition has inherent limitations as it uses a threshold to make assumptions about when qualitatively distinct water supply impacts arise, when in fact such impacts are likely to be more continuous and depend on locally relevant and context-specific factors. Moreover, this approach does not account for subannual snow season dynamics. With that said, in the midlatitudes of the American Cordillera, mountain runoff is often derived from snowpack<sup>50</sup> and is critically important to meet water demands. Post-emergence of low-to-no snow, annual runoff efficiency markedly declines throughout the midlatitudes of the American Cordillera, an indication that the definition conveys physically meaningful and decision-relevant information. The annual runoff declines are of the greatest magnitude during future dry years, though even wet years will see mountains generally becoming less efficient at generating runoff as the loss of snowpack enhances evaporative losses<sup>21</sup>. Decreased water availability from surface water in both dry and wet years yields two outcomes. First, future dry years will experience exacerbated drought conditions compared with historic dry years. Second, less efficient runoff in future wet years implies that these years will not

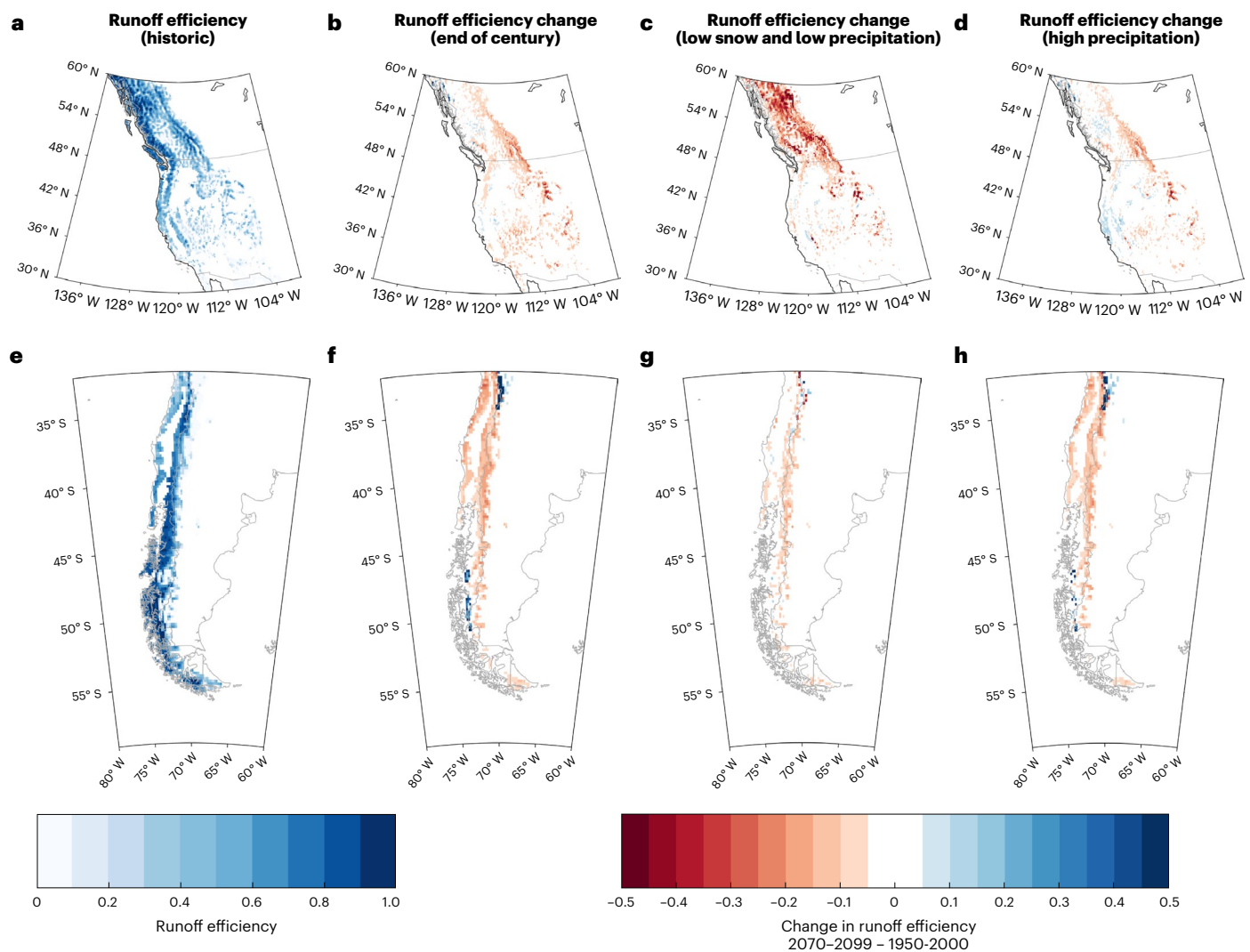


**Fig. 5 | Runoff efficiency declines post-emergence of low-to-no snow.** **a–h**, Spatial patterns of runoff efficiency for the northern hemisphere (30° N to 60° N; top row) and the southern hemisphere (32° S to 59° S; bottom row). In the northern hemisphere, runoff efficiency (the total annual runoff divided by the total annual precipitation) is determined from October through September of the following year. In the southern hemisphere, runoff efficiency is determined from January through December of the same year. Panels **a**, **e** show the historical

median annual runoff efficiency. Panels **b**, **f** show the change in runoff efficiency for the end of the century compared with the 1950–2000 historical reference period. Panels **c**, **g** show the same as **b**, **f** but for peak SWE and precipitation  $\leq 30$ th historical reference period percentile. Panels **d**, **h** show the same as **b**, **f** but for high-precipitation years ( $\geq 70$ th historical percentile). Country borders are indicated in grey.

ameliorate drought as effectively as occurred historically. However, increased runoff efficiency during occasional wet years in the coastal mountains of western North America and in the central Andes could provide brief drought amelioration provided this water can be stored<sup>16</sup>. Risks associated with markedly reduced runoff pose direct challenges to an already complex decision-making system<sup>5,7,16,18</sup>. These risks are heightened by centuries of infrastructure design and management strategies that have largely assumed climate stationarity and that do not agree with palaeoclimate records or future climate projections<sup>58–60</sup>. Further compounding these risks, the southern midlatitudes of the American Cordillera are projected to face low-to-no snow emergence nearly 20 years earlier than the northern midlatitudes. This warrants attention and action as the southern Chilean Andes have the highest global water tower index outside of Asia<sup>7</sup>, yet the region has notably less built infrastructure, fewer monitoring networks and fewer forecasting centres that could instil resilience to these hydrologic cycle alterations. The cross-hemispheric perspective of low-to-no snow emergence also demonstrates commonalities across regions

and highlights the need for a pro-active exchange of policy interventions<sup>61</sup>, cutting-edge water management strategies<sup>62–65</sup> and conceptual frameworks<sup>66,67</sup>. Most importantly, this perspective highlights the need to implement carbon mitigation strategies at scale<sup>68</sup> that inhibit the global warming level at which persistent low-to-no snow conditions emerge.

### Online content

Any methods, additional references, Nature Research reporting summaries, source data, extended data, supplementary information, acknowledgements, peer review information; details of author contributions and competing interests; and statements of data and code availability are available at <https://doi.org/10.1038/s41558-022-01518-y>.

### References

1. Körner, C., Paulsen, J. & Spehn, E. M. A definition of mountains and their bioclimatic belts for global comparisons of biodiversity data. *Alp. Bot.* **121**, 73–78 (2011).



2. Humboldt, A. v. & Bonpland, A. *Ideen zu einer Geographie der Pflanzen nebst einem Naturgemälde der Tropenländer* (Cotta, 1807).
3. Barry, R. G. *Mountain Weather and Climate* (Cambridge Univ. Press, 1992).
4. Paulsen, J. & Körner, C. A climate-based model to predict potential treeline position around the globe. *Alp. Bot.* **124**, 1–12 (2014).
5. Huss, M. et al. Toward mountains without permanent snow and ice. *Earth's Future* **5**, 418–435 (2017).
6. Smith, R. B. 100 years of progress on mountain meteorology research. *Meteorol. Monogr.* **59**, 20.1–20.73 (2019).
7. Immerzeel, W. W. et al. Importance and vulnerability of the world's water towers. *Nature* **577**, 364–369 (2020).
8. Bradley, R. S., Keimig, F. T. & Diaz, H. F. Projected temperature changes along the American Cordillera and the planned GCOS network. *Geophys. Res. Lett.* <https://doi.org/10.1029/2004GL020229> (2004).
9. Zappa, G., Ceppi, P. & Shepherd, T. G. Time-evolving sea-surface warming patterns modulate the climate change response of subtropical precipitation over land. *Proc. Natl Acad. Sci. USA* **117**, 4539–4545 (2020).
10. Payne, A. E. et al. Responses and impacts of atmospheric rivers to climate change. *Nat. Rev. Earth Environ.* **1**, 143–157 (2020).
11. Mooney, H., Dunn, E., Shropshire, F. & Song, L. Vegetation comparisons between the Mediterranean climatic areas of California and Chile. *Flora* **159**, 480–496 (1970).
12. di Castri, F. in *Mediterranean Type Ecosystems* (eds di Castri, F. & Mooney, H. A.) 21–36 (Springer, 1973).
13. Cody, M. L. & Mooney, H. A. Convergence versus nonconvergence in Mediterranean-climate ecosystems. *Annu. Rev. Ecol. Syst.* **9**, 265–321 (1978).
14. Morales, M. S. et al. Six hundred years of South American tree rings reveal an increase in severe hydroclimatic events since mid-20th century. *Proc. Natl Acad. Sci. USA* **117**, 16816–16823 (2020).
15. Viviroli, D., Kummerow, M., Meybeck, M., Kallio, M. & Wada, Y. Increasing dependence of lowland populations on mountain water resources. *Nat. Sustain.* <https://doi.org/10.1038/s41893-020-0559-9> (2020).
16. Siirila-Woodburn, E. et al. A low-to-no snow future and its impacts on water resources in the western United States. *Nat. Rev. Earth Environ.* **2**, 800–819 (2021).
17. Pepin, N. et al. Elevation-dependent warming in mountain regions of the world. *Nat. Clim. Change* **5**, 424–430 (2015).
18. Sturm, M., Goldstein, M. A. & Parr, C. Water and life from snow: a trillion dollar science question. *Water Resour. Res.* **53**, 3534–3544 (2017).
19. Saavedra, F. A., Kampf, S. K., Fassnacht, S. R. & Sibold, J. S. Changes in Andes snow cover from MODIS data, 2000–2016. *Cryosphere* **12**, 1027–1046 (2018).
20. Garreaud, R. D. et al. The Central Chile Mega Drought (2010–2018): a climate dynamics perspective. *Int. J. Climatol.* **40**, 421–439 (2020).
21. Milly, P. C. D. & Dunne, K. A. Colorado River flow dwindles as warming-driven loss of reflective snow energizes evaporation. *Science* **367**, 1252–1255 (2020).
22. Muñoz, A. A. et al. Water crisis in Petorca Basin, Chile: the combined effects of a mega-drought and water management. *Water* <https://doi.org/10.3390/w12030648> (2020).
23. Overpeck, J. T. & Udall, B. Climate change and the aridification of North America. *Proc. Natl Acad. Sci. USA* **117**, 11856–11858 (2020).
24. Serrano-Notivol, R. et al. Hydroclimatic variability in Santiago (Chile) since the 16th century. *Int. J. Climatol.* **41**, E2015–E2030 (2021).
25. Hock, R. et al. in *Special Report on the Ocean and Cryosphere in a Changing Climate* (eds Pörtner, H.-O. et al.) Ch. 2 (IPCC, Cambridge Univ. Press, 2019).
26. Held, I. M. & Soden, B. J. Robust responses of the hydrological cycle to global warming. *J. Clim.* **19**, 5686–5699 (2006).
27. Xu, Y. & Ramanathan, V. Latitudinally asymmetric response of global surface temperature: implications for regional climate change. *Geophys. Res. Lett.* <https://doi.org/10.1029/2012GL052116> (2012).
28. Friedman, A. R., Hwang, Y.-T., Chiang, J. C. & Frierson, D. M. Interhemispheric temperature asymmetry over the twentieth century and in future projections. *J. Clim.* **26**, 5419–5433 (2013).
29. Putnam, A. E. & Broecker, W. S. Human-induced changes in the distribution of rainfall. *Sci. Adv.* <https://doi.org/10.1126/sciadv.1600871> (2017).
30. Allan, R. P. et al. Advances in understanding large-scale responses of the water cycle to climate change. *Ann. N. Y. Acad. Sci.* **1472**, 49–75 (2020).
31. Amatulli, G. et al. A suite of global, cross-scale topographic variables for environmental and biodiversity modeling. *Sci. Data* **5**, 180040 (2018).
32. Shea, J. M., Whitfield, P. H., Fang, X. & Pomeroy, J. W. The role of basin geometry in mountain snowpack responses to climate change. *Front. Water* **3**, 4 (2021).
33. Patricola, C. M. et al. Maximizing ENSO as a source of western US hydroclimate predictability. *Clim. Dyn.* <https://doi.org/10.1007/s00382-019-05004-8> (2019).
34. Eidhammer, T., Grubišič, V., Rasmussen, R. & Ikdea, K. Winter precipitation efficiency of mountain ranges in the Colorado Rockies under climate change. *J. Geophys. Res. Atmos.* **123**, 2573–2590 (2018).
35. Lynn, E. et al. Technical note: precipitation-phase partitioning at landscape scales to regional scales. *Hydrol. Earth Syst. Sci.* **24**, 5317–5328 (2020).
36. Bales, R. C. et al. Mountain hydrology of the western United States. *Water Resour. Res.* <https://doi.org/10.1029/2005WR004387> (2006).
37. Jennings, K., Winchell, T. S., Livneh, B. & Molotch, N. P. Spatial variation of the rain–snow temperature threshold across the northern hemisphere. *Nat. Commun.* <https://doi.org/10.1038/s41467-018-03629-7> (2018).
38. Colombo, R. et al. Introducing thermal inertia for monitoring snowmelt processes with remote sensing. *Geophys. Res. Lett.* **46**, 4308–4319 (2019).
39. Demory, M. et al. The role of horizontal resolution in simulating drivers of the global hydrological cycle. *Clim. Dyn.* **42**, 2201–2225 (2013).
40. Rhoades, A. M., Ullrich, P. A. & Zarzycki, C. M. Projecting 21st century snowpack trends in western USA mountains using variable-resolution CESM. *Clim. Dyn.* **50**, 261–288 (2017).
41. Kapnick, S. B. et al. Potential for western US seasonal snowpack prediction. *Proc. Natl Acad. Sci. USA* **115**, 1180–1185 (2018).
42. Palazzi, E., Mortarini, L., Terzago, S. & Von Hardenberg, J. Elevation-dependent warming in global climate model simulations at high spatial resolution. *Clim. Dyn.* **52**, 2685–2702 (2019).
43. Haarsma, R. J. et al. High Resolution Model Intercomparison Project (HighResMIP v1.0) for CMIP6. *Geosci. Model Dev.* **9**, 4185–4208 (2016).
44. O'Neill, B. C. et al. The Scenario Model Intercomparison Project (ScenarioMIP) for CMIP6. *Geosci. Model Dev.* **9**, 3461–3482 (2016).
45. Körner, C. et al. A global inventory of mountains for bio-geographical applications. *Alp. Bot.* **127**, 1–15 (2017).
46. Conover, W. J. *Practical Nonparametric Statistics* Vol. 350 (John Wiley & Sons, 1999).

47. Woodhouse, C. A. & Pederson, G. T. Investigating runoff efficiency in Upper Colorado River streamflow over past centuries. *Water Resour. Res.* **54**, 286–300 (2018).
48. Lehner, F., Wahl, E. R., Wood, A. W., Blatchford, D. B. & Llewellyn, D. Assessing recent declines in Upper Rio Grande runoff efficiency from a paleoclimate perspective. *Geophys. Res. Lett.* **44**, 4124–4133 (2017).
49. Berghuijs, W., Woods, R. & Hrachowitz, M. A precipitation shift from snow towards rain leads to a decrease in streamflow. *Nat. Clim. Change* **4**, 583–586 (2014).
50. Li, D., Wrzesien, M. L., Durand, M., Adam, J. & Lettenmaier, D. P. How much runoff originates as snow in the western United States, and how will that change in the future? *Geophys. Res. Lett.* **44**, 6163–6172 (2017).
51. Livneh, B. & Badger, A. M. Drought less predictable under declining future snowpack. *Nat. Clim. Change* **10**, 452–458 (2020).
52. Trujillo, E. & Molotch, N. P. Snowpack regimes of the western United States. *Water Resour. Res.* **50**, 5611–5623 (2014).
53. Musselman, K. N., Clark, M. P., Liu, C., Ikeda, K. & Rasmussen, R. Slower snowmelt in a warmer world. *Nat. Clim. Change* **7**, 214–219 (2017).
54. Barnhart, T. B., Tague, C. L. & Molotch, N. P. The counteracting effects of snowmelt rate and timing on runoff. *Water Resour. Res.* **56**, e2019WR026634 (2020).
55. Bambach, N. E. et al. Projecting climate change in South America using variable-resolution Community Earth System Model: an application to Chile. *Int. J. Climatol.* <https://doi.org/10.1002/joc.7379> (2021).
56. Rhoades, A. M. et al. The shifting scales of western U.S. landfalling atmospheric rivers under climate change. *Geophys. Res. Lett.* **47**, e2020GL089096 (2020).
57. Rhoades, A. M., Risser, M. D., Stone, D. A., Wehner, M. F. & Jones, A. D. Implications of warming on western United States landfalling atmospheric rivers and their flood damages. *Weather Clim. Extrem.* **32**, 100326 (2021).
58. Milly, P. C. D. et al. Stationarity is dead: whither water management? *Science* **319**, 573–574 (2008).
59. Cosgrove, W. J. & Loucks, D. P. Water management: current and future challenges and research directions. *Water Resour. Res.* **51**, 4823–4839 (2015).
60. Fernández, A. et al. Dendrohydrology and water resources management in south-central Chile: lessons from the Río Imperial streamflow reconstruction. *Hydrol. Earth Syst. Sci.* **22**, 2921–2935 (2018).
61. Castilla-Rho, J., Rojas, R., Andersen, M., Holley, C. & Mariethoz, G. Sustainable groundwater management: how long and what will it take? *Glob. Environ. Change* **58**, 101972 (2019).
62. Scanlon, B. R., Reedy, R. C., Faunt, C. C., Pool, D. & Uhlman, K. Enhancing drought resilience with conjunctive use and managed aquifer recharge in California and Arizona. *Environ. Res. Lett.* **11**, 035013 (2016).
63. Sterle, K., Hatchett, B. J., Singletary, L. & Pohl, G. Hydroclimate variability in snow-fed river systems: local water managers' perspectives on adapting to the new normal. *Bull. Am. Meteorol. Soc.* **100**, 1031–1048 (2019).
64. Dillon, P. et al. Sixty years of global progress in managed aquifer recharge. *Hydrogeol. J.* **27**, 1–30 (2019).
65. Delaney, C. J. et al. Forecast informed reservoir operations using ensemble streamflow predictions for a multipurpose reservoir in Northern California. *Water Resour. Res.* **56**, e2019WR026604 (2020).
66. Szinai, J. K., Deshmukh, R., Kammen, D. M. & Jones, A. D. Evaluating cross-sectoral impacts of climate change and adaptations on the energy–water nexus: a framework and California case study. *Environ. Res. Lett.* **15**, 124065 (2020).
67. Vicuña, S. et al. in *Water Resources of Chile* (eds Fernández, B. & Gironás, J.) 347–363 (Springer International, 2021).
68. Williams, J. H. et al. Carbon-neutral pathways for the United States. *AGU Adv.* **2**, e2020AV000284 (2021).

**Publisher's note** Springer Nature remains neutral with regard to jurisdictional claims in published maps and institutional affiliations.

**Open Access** This article is licensed under a Creative Commons Attribution 4.0 International License, which permits use, sharing, adaptation, distribution and reproduction in any medium or format, as long as you give appropriate credit to the original author(s) and the source, provide a link to the Creative Commons license, and indicate if changes were made. The images or other third party material in this article are included in the article's Creative Commons license, unless indicated otherwise in a credit line to the material. If material is not included in the article's Creative Commons license and your intended use is not permitted by statutory regulation or exceeds the permitted use, you will need to obtain permission directly from the copyright holder. To view a copy of this license, visit <http://creativecommons.org/licenses/by/4.0/>.

© The Author(s) 2022

## Methods

### HighResMIP v.1.0

The HighResMIP ensemble offers cutting-edge, high-resolution Earth system model simulations, particularly over centennial-scale periods. The model horizontal resolutions across the three models used in our analysis spanned ~250 km to ~20 km (Supplementary Table 1). The only model to satisfy Tier 1–3 HighResMIP protocols (MRI-AGCM3-2) was used for a more extensive analysis of the date of and degrees to emergence of low-to-no snow and its post-emergence implications for the mountainous hydrologic cycle (Supplementary Information). MRI-AGCM3-2 also provided some of the highest-resolution simulations (60 km and 20 km) in the HighResMIP ensemble and has shown above-median skill (total score, 82; top score, 85) across several Earth system model skill indicators, spanning the energy budget, hydrologic cycle, large-scale dynamics and seasonal metrics<sup>69</sup>. The MRI-AGCM3-2 snow model has four layers and prognostic snow density that accounts for mixed-phase water storage and transport, densification, and albedo changes between fresh and aged snow<sup>70</sup>. Furthermore, MRI-AGCM3-2 relies on both surface air temperature and, unlike most Earth system models, relative humidity to determine rain–snow partitioning in its land-surface model (see Section 2.3 and Appendix C/D in Hirai et al.<sup>70</sup>). Jennings et al.<sup>37</sup> have shown that this can have an outsized role in the representation of the 50% rain–snow temperature threshold, where a 10% increase in relative humidity decreases the 50% rain–snow temperature threshold by 0.8 °C. This is particularly important for snow accumulation in continental mountain regions (with lower relative humidity) and has been identified as a major model development goal to enhance Earth system model fidelity in mountains (see Box 1 in Siirila-Woodburn et al.<sup>16</sup>).

There is a growing literature that shows that Earth system model simulations run at sufficiently high resolution ( $\leq 0.5^\circ$  horizontal resolution), like those provided by HighResMIP, show better convergence in the representation of the global hydrologic cycle, generally through better representation of topography, moisture transport, land–sea contrasts, and evapotranspiration and moisture convergence to precipitation ratios, and less reliance on subgrid-scale parameterizations to estimate precipitation<sup>39</sup>. For example, enhanced topographic representation along the American Cordillera (namely, in Central America) has also been shown to dampen long-standing global circulation biases, such as the double Intertropical Convergence Zone<sup>71</sup>, and has shown better representation in mountain-range-scale snowpack life cycles than low-resolution simulations<sup>40,41,72</sup>. Although model convergence in the representation of the seasonal cycle of mountain snowpack may require even higher resolutions, we also note that model fidelity does not always systematically increase with higher resolution alone<sup>72</sup>.

With that said, the analysis was limited by the lack of Earth system models that simulated a future climate scenario to 2100 and output daily SWE to appropriately estimate the peak amount and timing of water stored in mountain snowpacks. The weak signal-to-noise ratio in changing snow conditions (that is, the climate change signal versus the noise of interannual variability) along the American Cordillera by 2050 and the stronger signal-to-noise ratio post-2050 underscore the importance of producing continuous climate projections to at least 2100 in future HighResMIP ensembles. Therefore, a major limitation of this analysis is that we were constrained to using a single model to estimate the date of and degrees to emergence of low-to-no snow. The use of a single-member, single-model simulation does not allow for the assessment of uncertainty in future projections associated with intermodel structural and parameter uncertainty, such as climate sensitivity or internal variability, and how they might influence estimates of a low-to-no snow future<sup>73–75</sup>. A prioritization of multiple ensemble members in future HighResMIP experiments would help constrain uncertainties associated with internal variability and climate sensitivity. Uncertainty in our analysis also arises due to the use of a single emissions scenario, which does not account for rapid policy intervention that could limit greenhouse gas emissions<sup>68</sup>. To sidestep emission-scenario-specific outcomes, we

explicitly highlight both the global and local surface air temperatures at which low-to-no snow emergence might occur. With all of that said, we note that our analysis is a proof of concept of what future high-resolution multi-model ensembles could deliver.

### Mountain definition

To evaluate how well the hypsometry of the American Cordillera is represented in the model simulations and assess the mountainous hydrologic cycle response to future asymmetric hemispheric warming, we utilize a mountain mask that isolates the world's mountains into 1,013 distinct polygons comprising an area of 13.8 million km<sup>2</sup> (refs. 1,45). We subset this larger mountain mask to include only the American Cordillera, which spans the Pacific Coast ranges of Alaska and British Columbia through the South American Andes (Supplementary Fig. 16). The American Cordillera is ideal for assessing hemispheric asymmetry of low-to-no snow, as it is contiguous across more latitude bands than any mountain range in the world and is continuously abutted by the Pacific Ocean to its west, ensuring that hydrologic cycle responses are not markedly influenced by upwind landmass interactions, save for the interior mountain ranges of the northern hemisphere midlatitudes.

According to the Global Mountain Biodiversity Assessment (<http://www.mountainbiodiversity.org/explore>), devised by Körner et al.<sup>45</sup>, the American Cordillera comprises a mean latitudinal elevation between 83 m and 3,498 m, a maximum latitudinal elevation of 6,261 m (based on the ~4-km-resolution Shuttle Radar Topography Mission elevation dataset) and a maximum ruggedness of 1,154 m (the maximal elevational difference in a 3 × 3 grid). The highest-resolution model in the HighResMIP ensemble (MRI-AGCM3-2-S) has nearly the same representation of the mean latitudinal elevation (between 28 m and 3,497 m) as the Global Mountain Biodiversity Assessment, yet there is a ~1,000 m low bias in the maximum latitudinal elevation of 5,294 m (Supplementary Fig. 16).

### Calculation of the date of emergence of low-to-no snow

To assess the hemispheric asymmetry and latitudinal responses of the American Cordillera to climate change, we assess the annual maximum SWE, or peak SWE. Peak SWE is calculated for the entirety of the HighResMIP model simulation period (1950–2099) and averaged across each latitude band within the American Cordillera. To eliminate regions of ephemeral snow cover, a minimum amount of peak SWE depth was needed (>2.54 mm, or the instrumental precision of in situ SWE measurements; <https://www.nrcs.usda.gov/wps/portal/wcc/home/dataAccessHelp/faqs/snotelSensors/>). We then bin filtered the peak SWE estimates into 10th-percentile bins, using the first 50 years of the simulation as the historical reference period (1950–2000). Importantly, this historical reference period is characterized by a wide range of climate variability indicators (for example, strong to weak phases of the El Niño Southern Oscillation, as shown in Patricola et al.<sup>33</sup>).

To quantitatively isolate the persistence of low-to-no snow years, we develop several definitions and apply them to the HighResMIP simulation over the American Cordillera. Low-snow is defined as peak SWE  $\leq 30$ th percentile, and (virtually) no snow is peak SWE  $\leq 10$ th percentile<sup>16</sup>. These percentiles are also analogous to “snow drought” thresholds utilized in recent literature<sup>76–78</sup>, but we opt for the low-to-no snow terminology because drought implies a temporary deviation from average that is unlikely to occur in a continuously warming world. The low-to-no snow percentile-based definition is chosen partly on the basis of the success of the United States Drought Monitor's ability to highlight impactful water stress on ecologic and socio-economic systems using percentile-based thresholds<sup>77,79</sup> and, more specifically, on the basis of recent research showing that runoff is reduced and consistently more constrained in portions of the western United States when peak SWE approaches conditions of low-to-no snow<sup>78,80</sup>. Peak SWE is used as a proxy for the total water volume available for downstream reservoir replenishment and water availability. The use of peak SWE also gets around arbitrary dates often used in resource management (for



example, 1 April) that cannot account for earlier shifts in peak SWE timing with warming, nor can these dates be applied across hemispheres.

We define a back-to-back low-to-no snow year as ‘extreme’, five years in a row as ‘episodic’ and ten years in a row as ‘persistent’. These temporal definitions are chosen on the basis of their historical impact on water management—namely, the ability of traditional management mechanisms and infrastructure storage capacities to meet annual water demand<sup>16</sup>. Back-to-back (extreme) years of low-to-no snow have occurred in the historical record (for example, in the 1970s and 2010s)<sup>81,82</sup>. Although impactful, historically these conditions were intermittent and not spatially ubiquitous across the western United States, rarely leading to catastrophic water supply outcomes. Episodic low-to-no snow (five years in a row) has also occurred in recent history (2012–2016) in the western US and led to dramatic shifts in water and agricultural management practices, new water policy (for example, the Sustainable Groundwater Act) and mandatory reductions in water use<sup>83</sup>. Persistent low-to-no snow (ten years in a row) has yet to occur in the historical record. In such a case, it would probably be virtually impossible to meet historical water demand assuming no changes to water management practices and infrastructure.

Using both the low-to-no snow definition and the temporal definitions, we then estimate, at each latitude band (mean conditions) along the American Cordillera, when peak SWE percentiles meet (assigned a 1) or don’t meet (assigned a 0) the  $\leq 30$ th percentile. Then, for years with low-to-no snow, we identify instances with at least one (for ‘extreme’), at least four (for ‘episodic’), or at least nine (for ‘persistent’) consecutive preceding years of low-to-no snow conditions. The end result is a time series of zeros and ones in each latitude band describing the non-occurrence or occurrence (respectively) of each low-to-no snow condition in each year. A common statistical analysis when dealing with 0-and-1 data such as the low-to-no snow categories is that of logistic regression, which seeks to quantify relationships between some independent or explanatory variable of interest (for example, surface air temperature in each year) and a dependent or response variable that is {0, 1}. Unlike ordinary least squares regression, which quantifies linear relationships between an explanatory variable and a continuous response variable, logistic regression quantifies a relationship between an arbitrary explanatory variable and the probability of the response variable being 1. Numerical methods are used to estimate the various statistical parameters involved in the logistic regression model (Supplementary Information), which can then be used to derive best estimates of how the probability of experiencing a low-to-no snow category evolves over time according to surface air temperature. We then use these fitted probabilities to identify a date of emergence for each low-to-no snow category by selecting the first year for which the estimated probability exceeds 0.5. The 0.5 threshold is chosen because it represents at least a greater-than-random chance of occurrence of the various consecutive low-to-no snow year conditions.

## Data availability

The post-processed data used in this analysis are available via a publicly accessible Science Gateway at the US Department of Energy’s NERSC ([https://portal.nersc.gov/archive/home/a/arhoades/Shared/www/NCC\\_2022](https://portal.nersc.gov/archive/home/a/arhoades/Shared/www/NCC_2022)).

## Code availability

The analysis code for this study is available via a publicly accessible Science Gateway at the US Department of Energy’s NERSC ([https://portal.nersc.gov/archive/home/a/arhoades/Shared/www/NCC\\_2022](https://portal.nersc.gov/archive/home/a/arhoades/Shared/www/NCC_2022)).

## References

69. Fasullo, J. T. Evaluating simulated climate patterns from the CMIP archives using satellite and reanalysis datasets using the Climate Model Assessment Tool (CMATv1). *Geosci. Model Dev.* **13**, 3627–3642 (2020).
70. Hirai, M. et al. Development and validation of a new land surface model for JMA’s operational global model using the CEOP observation dataset. *J. Meteorol. Soc. Japan II* **85A**, 1–24 (2007).
71. Baldwin, J. W., Atwood, A. R., Vecchi, G. A. & Battisti, D. S. Outside influence of Central American orography on global climate. *AGU Adv.* **2**, e2020AV000343 (2021).
72. Rhoades, A. M. et al. Sensitivity of mountain hydroclimate simulations in variable-resolution CESM to microphysics and horizontal resolution. *J. Adv. Model. Earth Syst.* **10**, 1357–1380 (2018).
73. Hawkins, E. & Sutton, R. The potential to narrow uncertainty in regional climate predictions. *Bull. Am. Meteorol. Soc.* **90**, 1095–1108 (2009).
74. Hawkins, E., Smith, R. S., Gregory, J. M. & Stainforth, D. A. Irreducible uncertainty in near-term climate projections. *Clim. Dyn.* **46**, 3807–3819 (2016).
75. Lehner, F. et al. Partitioning climate projection uncertainty with multiple large ensembles and CMIP5/6. *Earth Syst. Dyn.* **11**, 491–508 (2020).
76. Marshall, A. M., Abatzoglou, J. T., Link, T. E. & Tennant, C. J. Projected changes in interannual variability of peak snowpack amount and timing in the western United States. *Geophys. Res. Lett.* **46**, 8882–8892 (2019).
77. Huning, L. S. & AghaKouchak, A. Global snow drought hot spots and characteristics. *Proc. Natl Acad. Sci. USA* **117**, 19753–19759 (2020).
78. Hatchett, B. J., Rhoades, A. M. & McEvoy, D. J. Monitoring the daily evolution and extent of snow drought. *Nat. Hazards Earth Syst. Sci.* **22**, 869–890 (2022).
79. Svoboda, M. et al. The Drought Monitor. *Bull. Am. Meteorol. Soc.* **83**, 1181–1190 (2002).
80. Sextone, G. A., Driscoll, J. M., Hay, L. E., Hammond, J. C. & Barnhart, T. B. Runoff sensitivity to snow depletion curve representation within a continental scale hydrologic model. *Hydrol. Process.* **34**, 2365–2380 (2020).
81. Mote, P. W., Li, S., Lettenmaier, D. P., Xiao, M. & Engel, R. Dramatic declines in snowpack in the western US. *NPJ Clim. Atmos. Sci.* **1**, 2 (2018).
82. Huning, L. S. & AghaKouchak, A. Approaching 80 years of snow water equivalent information by merging different data streams. *Sci. Data* **7**, 333 (2020).
83. Mote, P. W. et al. Perspectives on the causes of exceptionally low 2015 snowpack in the western United States. *Geophys. Res. Lett.* **43**, 10980–10988 (2016).

## Acknowledgements

The Director, Office of Science, Office of Biological and Environmental Research of the US Department of Energy Regional and Global Climate Modeling Program (RGCM) through ‘the Calibrated and Systematic Characterization, Attribution and Detection of Extremes (CASCADE)’ Science Focus Area (award no. DE-AC02-05CH11231) funded A.M.R., M.D.R., W.D.C., P.A.U. and M.F.W., and the ‘Integrated Evaluation of the Simulated Hydroclimate System of the Continental US’ project (award no. DE-SC0016605) funded A.M.R., R.M., P.A.U., C.M.Z. and A.D.J. B.J.H. was supported by the Maki Foundation and the California Department of Water Resources. E.R.S.-W. was funded by the Watershed Function Scientific Focus Area funded by the US Department of Energy, Office of Science, Office of Biological and Environmental Research (award no. DE-AC02-05CH11231). The analysis and model simulations were analysed using resources of the National Energy Research Scientific Computing Center (NERSC), a US Department of Energy Office of Science User Facility located at Lawrence Berkeley National Laboratory, operated under Contract No. DE-AC02-05CH11231. We acknowledge the World Climate Research Programme, which, through



its Working Group on Coupled Modelling, coordinated and promoted CMIP6. We thank the climate modelling groups for producing and making available their model output, the Earth System Grid Federation (ESGF) for archiving the data and providing access, and the multiple funding agencies who support CMIP6 and ESGF. We also thank the US Department of Energy's RGMA programme area, the Data Management programme and NERSC for making this coordinated CMIP6 analysis activity possible. We especially thank M. Bukovsky for help in obtaining the SA-CORDEX data from the [esgf-ictp.hpc.cineca.it](http://esgf-ictp.hpc.cineca.it) server.

### Author contributions

A.M.R. conceived the study and led all analyses, figure generation and writing. B.J.H., M.D.R. and A.D.J. supported the analyses, writing and figure generation. W.D.C. garnered and curated the data. All authors contributed to the interpretation of the study results and editing of the manuscript and figures.

### Competing interests

The authors declare no competing interests.

### Additional information

**Supplementary information** The online version contains supplementary material available at <https://doi.org/10.1038/s41558-022-01518-y>.

**Correspondence and requests for materials** should be addressed to Alan M. Rhoades.

**Peer review information** *Nature Climate Change* thanks Alfonso Fernández, Isabel Hoyos, Noah Molotch and Pablo Zaninelli for their contribution to the peer review of this work.

**Reprints and permissions information** is available at [www.nature.com/reprints](http://www.nature.com/reprints).